

The primary aim of this study is to identify all possible conformers of halomon and their relative stability is determined by using DFT calculation. The structure of most stable conformer is compared with the experimental values. Finally harmonic vibrational frequency calculations were performed at the B3LYP / 6-31+G(d,p) level.

8.2. Computational methods

The initial structure of halomon was obtained from Cambridge Crystallographic Data Centre (www.ccdc.cam.ac.uk) and other conformations are constructed by molecular dynamics calculations using the PM7 semi-empirical potential, followed by a geometry optimization using the same semi-empirical method. The molecular dynamics simulations were done using the Velocity Verlet algorithm and other default settings were used. Similar geometries were omitted (two geometries are considered similar if the difference between their energies is less than 1 kJ/mol). The conformational isomers of halomon obtained from the PM7 semi-empirical calculations were fully re-optimized by using the DFT/B3LYP method with 6-31+G(d,p) basis set to determine the relative energies and the structures of five distinct conformations. Vibrational analysis was carried out to ensure that each optimization located a true minimum energy structure (no imaginary frequencies). Semi-empirical calculations were done by MOPAC2016 [9]. The DFT calculations were performed with the Firefly [10].

8.3. Results and discussion

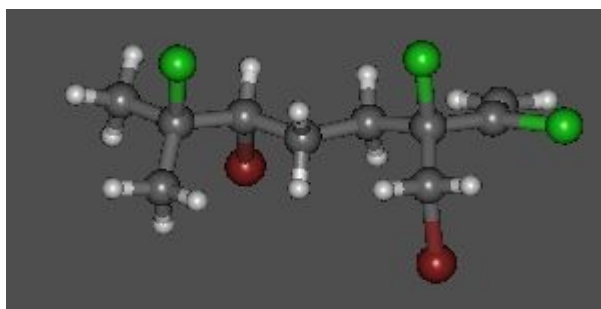
During the DFT optimization, some conformations are converted into the most stable conformers. Table 8.1 shows the total and relative energies of the five conformers of halomon calculated by the DFT B3LYP/6-31+G(d,p).

Table 8.1. DFT calculated energies of the various conformers of halomon and the relative energies with respect to the most stable conformation

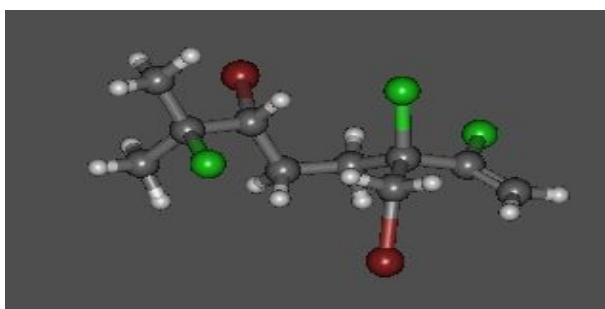
Conformer	a	b	c	d	e
Total energy ^a	-6914.2546	-6914.2509	-6914.2505	-6914.2471	-6914.2465
Relative energy ^b	0.00	9.71	10.76	19.69	21.27

^aThe unit of DFT energy is in a.u. ^bThe unit of relative energy is (kJ/mol)

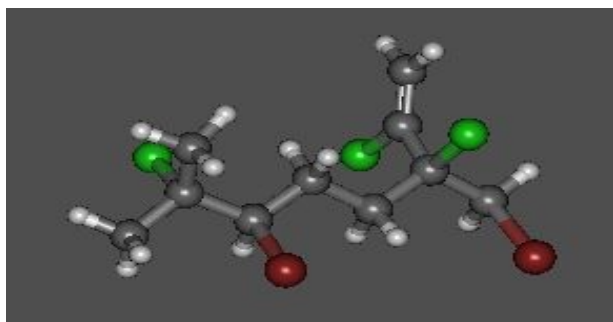
Table 8.1 suggest that conformer a is 9.71 kJ/mol more stable than conformer b, about 10.76 kJ/mol more stable than conformer c, about 19.69 kJ/mol more stable than conformer d and 21.27 kJ/mol more stable than conformer e, respectively. Figure 8.2 shows the DFT B3LYP/6-31+G(d,p) optimized stable structures of the various conformers of halomon. The molecular plots were produced using Gabedit 2.4.8 [11].



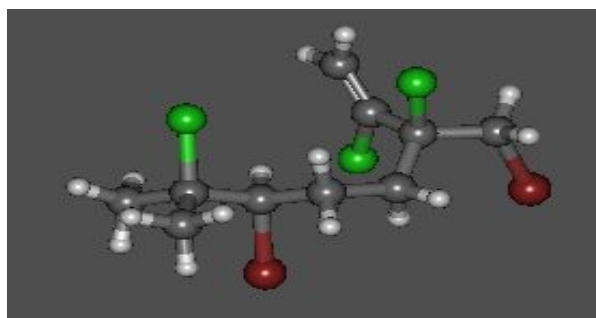
a



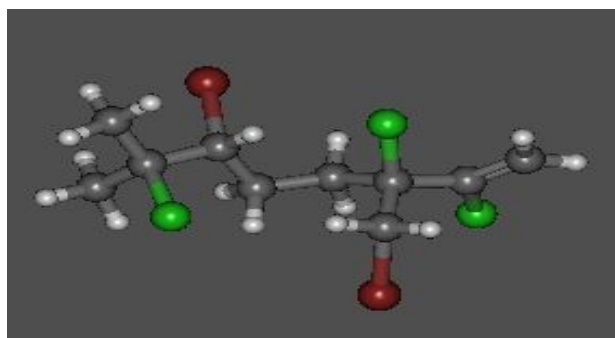
b



c



d



e

Figure 8.2. Conformers of halomon

The calculated bond lengths, bond angles and dihedral angles of most stable conformer of halomon (a) by B3LYP/6-31+G(d,p) and B3PW91/6-31+G(d,p) are listed in Table 8.2 along with the experimental data obtained by X-ray crystal analysis. The comparison between the theoretical and experimental data on bond lengths, bond angles and dihedral angles in Table 8.2 shows a good agreement between them. In the experiments, the shortest bond in halomon was observed for C1-C2 while the longest bonds are C9-Br13 and C6-Br14. Our theoretical results confirm these experimental findings as shown in Table 8.2.

Table 8.2. Optimized structural parameters of most stable conformer of halomon with experimental data

Structural parameters	Experimental	B3LYP/6-31+G(d,p)	B3PW91/6-31+G(d,p)
Bond length (Å)			
C1-C2	1.388	1.333	1.332
C2-C3	1.517	1.520	1.517
C3-C4	1.388	1.540	1.534
C4-C5	1.495	1.536	1.530
C5-C6	1.570	1.527	1.522

Table 8.2 (continued)

Bond length (Å)	Experimental	B3LYP/6- 31+G(d,p)	B3PW91/6- 31+G(d,p)
C6-C7	1.624	1.548	1.544
C7-C8	1.503	1.528	1.523
C3-C9	1.582	1.531	1.527
C7-C10	1.500	1.530	1.525
C2-Cl11	1.718	1.767	1.753
C3-Cl12	1.818	1.869	1.845
C9-Br13	2.002	1.970	1.949
C6-Br14	1.985	2.005	1.981
C7-Cl15	1.854	1.872	1.894
Bond angle (°)			
C1-C2-C3	123.40	126.26	126.08
C2-C3-C4	117.34	112.00	111.93
C3-C4-C5	115.45	114.90	114.69
C4-C5-C6	113.23	112.60	112.46
C5-C6-C7	113.57	116.38	116.19
C6-C7-C8	106.60	112.68	112.40
C1-C2-Cl11	115.94	118.29	118.59
C2-C3-Cl12	105.66	107.23	107.42
C9-C3-Cl12	99.88	103.31	103.62
C3-C9-Br13	109.81	110.65	110.44
C7-C6-Br14	105.16	108.93	109.07
C6-C7-Cl15	100.28	104.15	104.32

Table 8.2 (continued)

Dihedral angles ($^{\circ}$)	Experimental	B3LYP/6-31+G(d,p)	B3PW91/6-31+G(d,p)
C1-C2-C3-Cl12	-118.53	-113.57	-113.60
C4-C3-C9-Br13	58.53	63.46	64.15
C5-C6-C7-Cl15	100.28	66.00	65.73
Br14-C6-C7-Cl15	-178.26	-171.08	-178.95
Cl12-C3-C9-Br13	-177.39	-179.12	-171.08

The main differences are the torsion angle formed by C5-C6-C7-Cl15 atoms (100.28° in crystallography, 66.00° in B3LYP and 65.73° in B3PW91) and these differences are probably due to packing effects. The IR spectra for the most stable conformer of halomon are given in Figure 8.3.

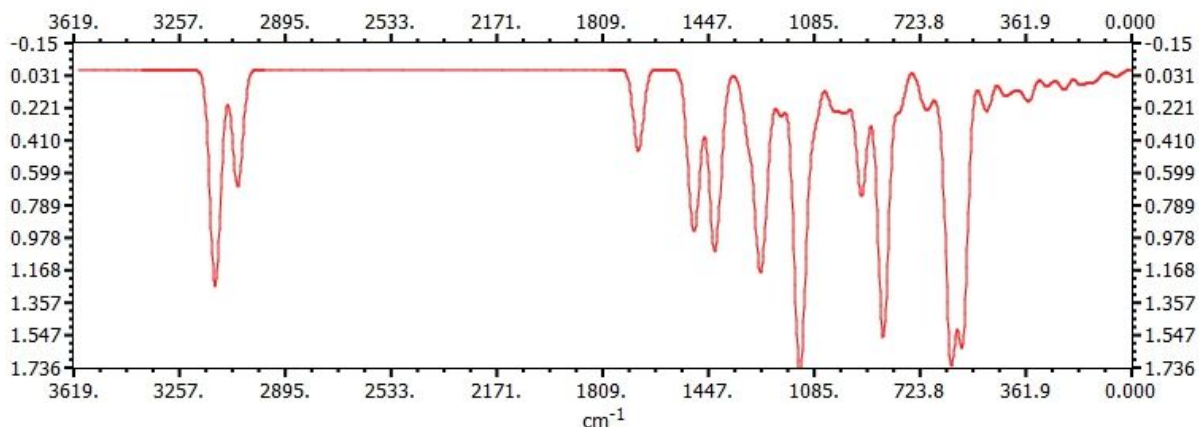


Figure 8.3. IR spectra of the most stable conformer of Halomon in gas phase

Due to the use of the harmonic approximation and incomplete inclusion of electron correlation computed harmonic vibrational frequencies are usually somewhat larger than experimental fundamentals. The B3LYP/6-31G+(d,p) spectra show C-H stretching modes in the 3000-3200 cm^{-1} range.

8.4. Conclusions

The present quantum chemical investigation based on DFT methods provide useful information about the structure of halomon. The harmonic vibrational frequencies for halomon were calculated at the B3LYP/6-31+G(d,p).

8.5. Reference

- [1] R.W. Fuller, J.H. Cardellina II, Y. Kato, L.S. Brinen, J. Clardy, K.M. Snader, M.R. Boyd, A pentahalogenated monoterpene from the red alga *Portieria hornemannii* produces a novel cytotoxicity profile against a diverse panel of human tumor cell lines, *J Med Chem.* 35 (1992) 3007-3011.
- [2] R.W. Fuller, J.H. Cardellina II, J. Jurek, P.J. Scheuer, B.A. Lindner, M. McGuire, G.N. Gray, J.R. Steiner, J. Clardy, E. Menez, R.H. Shoemaker, D.J. Newman, K.M. Snader, M.R. Boyd, Isolation and structure/activity features of halomon - related antitumor monoterpenes from the red alga *Portieria hornemannii*, *J Med Chem.* 37 (1994) 4407-4411.
- [3] M.J. Egorin, D.L. Sentz, D.M. Rosen, M.F. Ballesteros, C.M. Kearns, P.S. Callery, J.L. Eiseman, Plasma pharmacokinetics, bioavailability, and tissue distribution in CD₂F₁ mice of halomon, an antitumor halogenated monoterpene isolated from the red alga *Portieria hornemannii*, *Cancer Chemother Pharmacol.* 39 (1996) 51-60.
- [4] M.J. Egorin, M.D. Rosen, S.E. Benjamin, P.S. Callery, D.L. Sentz, J.L. Eiseman, In vitro metabolism of mouse and human liver preparations of halomon, an antitumor halogenated monoterpene, *Cancer Chemother Pharmacol.* 41 (1997) 9-14.

- [5] M.E. Jung, M.H. Parker, Synthesis of several naturally occurring polyhalogenated monoterpene of the halomon class, *J Org Chem.* 62 (1997) 7094-7095.
- [6] T. Sotokawa, T. Noda, S. Pi, M.A. Hirama, A three step synthesis of halomon, *Angew Chem Int Ed Engl.* 39 (2000) 3430-3432.
- [7] H.D. Yoo, S.O. Ketchum, D. France, K. Bair, W.H. Gerwick, Vidalenolone , a novel phenolic metabolite from the tropical red alga *Vidalia* sp., *J Nat Prod.* 65 (2002) 51-53.
- [8] E.H. Andrianasolo, D. France, S.C. Kennon, W.H. Gerwick, DNA Methyl Transferase Inhibiting Halogenated Monoterpenes from the Madagascar Red Marine Alga *Portieria hornemannii*, *J Nat Prod.* 69 (2006) 576-579.
- [9] J.J.P. Stewart, MOPAC2016, Stewart Computational Chemistry, Colorado Springs, CO, USA, [HTTP://OpenMOPAC.net](http://OpenMOPAC.net) (2016).
- [10] A.A. Granovsky, Firefly version 8, [www http://classic.chem.msu.su/gran/firefly/index.html](http://classic.chem.msu.su/gran/firefly/index.html).
- [11] A.R. Allouche, Gabedit-a graphical user interface for computational chemistry softwares, *J Comput Chem.* 32 (2011) 174-182.